Journal of Robotic Systems, 14(7):545-557

A Control Basis for Learning Multifingered Grasps

Jefferson A. Coelho, Jr. and Roderic A. Grupen
Laboratory for Perceptual Robotics
Department of Computer Science
University of Massachusetts at Amherst

October 24, 1997

Abstract

In this paper, we introduce a robust controller that uses contact position and normal feedback to generate contact configurations for statically stable grasps. The approach uses a context sensitive composition of two controllers that minimize force and moment residuals in the grasp configuration. We show that equilibria in the composite controller correspond to optimal contact configurations for 2 and 3 contacts on regular, convex polygons. The preimage is used to generalize the controller to arbitrary object geometries by learning a policy for compensation and to address object recognition, and contact (de)allocation.

1 Introduction

Grasping and manipulation tasks with dextrous hands introduce formidable challenges to traditional planning and control techniques. These tasks include a broad range of contexts; dextrous hands are expected to be flexible with respect to varying object geometry, the hand mechanism itself is highly redundant, and the environments in which they are expected to operate are uncertain and unstructured. This paper concerns the process of generating statically stable multifingered grasp configurations on-line. Our approach is to cast grasp synthesis as a control problem — that is, we will propose that grasp formation can be posed as a closed-loop response to contact feedback. We show that statically stable grasps can be formed for some classes of objects without *a priori* models of the object's surface geometry. Continuous sensor feedback also addresses uncertainty and/or imprecision during the execution of a grasp. Such a model for reflexive grasp formation is capable of alleviating significant computational burden related to model building and grasp planning, and provides a mechanism for executing grasp plans when they exist.

In this paper, grasping is formulated as a *robust* control problem wherein variations in object geometry and contact friction properties are modeled as *disturbances.* The grasp controller is designed to be robust to these forms of variations in the plant. This approach produces statically stabilizable contact configurations for 2 and 3 contact grasps on convex, regular polygons, and it is robust with respect to specified variations in the object geometry. To address general object geometries, the *preimage* of the grasp controller is constructed to associate the expected quality of equilibrium grasp configurations with precursor grasp states. The quality metric selected is the minimum coefficient of friction required to stabilize the grasp, and therefore extends the approach to a richer class of contact types. This representation is used to support an adaptive control compensator and a means of contact (de)allocation. In addition, we show how the stream of contact data gathered during grasp formation can be used to resolve object identity within a set of candidate objects.

2 Related Work

In 1982, Salisbury employed the grip Jacobian, G, to transform contact forces to object frame wrenches [1]. Since that time, the issue of constructing appropriate contact configurations (and therefore, grip Jacobians) has received a great deal of attention. This issue we will refer to as the grasp synthesis problem. It may be viewed as a search in contact configuration space for configurations that can transmit the right set of wrenches to the object. Most work in this regard concerns off-line grasp synthesis, in which the search is conducted to position a pre-specified number of contacts on a model of the object. Previous work in off-line grasp synthesis may be categorized into two broad categories.

- Optimization techniques have been used to explore the contact configuration space, especially the subset of configurations satisfying the force closure condition. *Force closure* requires that the contact configuration describe a convex set in wrench space containing the origin and that all contact forces are strictly positive and within their respective friction cones. The evaluation function to be optimized measures the relative utility of grasp configurations based on several possible attributes. In the work of Faverjon and Nguyen [2, 3], the set of contact configurations that satisfy the force closure condition are further sorted on the basis of precision requirements. Sorting may also be based on the maximum force required to nullify the worst case wrench [4].

  Other evaluation functions incorporate the manipulability of the resulting grasp configuration [5], its reliance on frictional forces [6], and the ability of the grasp to resist external disturbances [7, 8]. In these broader contexts, the complexity of optimization-based approaches can be prohibitive.

- Taxonomy-based grasp synthesis observes that grasp geometry is strongly related to hand morphology. Taking cues from human grasping strategies (described in detail by Napier [9]), these techniques relate hand configuration (and thus contact configuration) to the geometry of the object in the context of the task [10, 11, 12]. This approach is a memory-intensive map from object geometry and task to appropriate hand configuration and pose.

  Pollard [13] proposed an approach in which grasp prototypes are generalized offline and indexed according to task and grasp quality. The grasp prototype can be used later to constrain an online search of grasp configurations for novel objects.

These approaches can be distinguished on the basis of object geometries permitted (polygons, parametric surfaces, two and three dimensions), and on the basis of the type and number of contacts permitted. All depend on complete *a priori* information concerning object geometry and, in some cases, friction coefficients between fingers and object.

Besides Pollard, that reports a fast online search procedure capable of adapting grasp prototypes to new objects, only the Jameson and Leifer [8] present a grasp strategy that is adaptable. Their procedure uses artificial potential fields to satisfy joint range and interference constraints as the physical manipulator grasps an object. Few approaches address the online grasp synthesis problem. Most sensor-based approaches related to grasping are vision-based [14, 15]; typically, geometric parameters extracted from the object image are used to predict grasp quality. An open loop control scheme is used during grasping, and learning procedures are employed to build the map from visual features to expected grasp quality indices. Tactile-based grasp procedures often address the stability maintenance problem [16], in which contact forces are modulated to maintain the contact forces within the friction cone. We know of no other techniques in the literature for haptically-driven grasp synthesis.

3 Grasp Synthesis as a Feedback Control Problem

Figure 1 depicts the closed-loop control scheme proposed. The plant consists of an k-contact grasp configuration on an unknown object geometry. Conceptually, the plant transforms a contact configuration into an object wrench. The grasp controller determines how to apply inputs to the plant to achieve a reference wrench. Control is designed to be robust with respect to a broad range of possible plants.

The feedback controller relies on a frictionless point contact model represented by a unit force oriented along the inward directed surface normal. Sensor evidence in the form of contact positions and normals is used to construct the instantaneous grip Jacobian, G, with which contact forces are transformed into object frame wrenches. This local characterization captures the ability of the object surface to carry contact forces and to generate object frame wrenches.

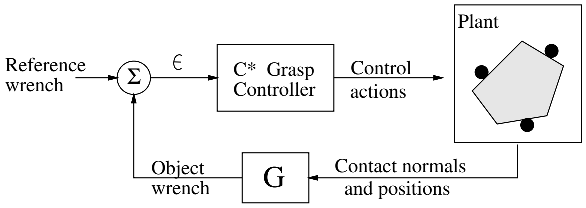

Figure 1: Grasp synthesis as a control problem.

A grasp configuration is considered statically stabilizable if the grip Jacobian, G, contains a null space consisting of wrenches derived from strictly positive-sense contact forces. The controller constructs the grasp configuration by continuously adjusting the contact coordinates to achieve a reference net wrench. If there exists a contact wrench that can be written as a positive linear combination of other contact wrenches, $\omega_i = \sum_{j \neq i} \omega_j$, then the object may be *squeezed* within a null space of the grip Jacobian without applying a net wrench to the object. It follows that the condition $\sum \omega_i = 0$ is a necessary condition for stable grasp configurations, and the corresponding control reference is a zero net wrench.

The feedback error ϵ in Figure 1 is defined as the squared magnitude of the net object frame wrench.

$$\begin{aligned} \epsilon &= \vec{\rho}^{\,T} \vec{\rho} \\ &= \left(\frac{1}{k} \sum_{i=1}^{k} \vec{\omega_i} \right)^T \left(\frac{1}{k} \sum_{i=1}^{k} \vec{\omega_i} \right), \end{aligned} \tag{1}$$

where $\vec{\rho}$ is the normalized wrench residual and expresses the net wrench over k contacts, and $\vec{\omega_i}$ is the wrench resulting from the i^{th} contact force.

The squared residual, ϵ, is minimized by following the negative gradient of ϵ with respect to the contact configuration. One can compute $\frac{\partial \epsilon}{\partial \theta_i}$:

$$\begin{aligned} \frac{\partial \epsilon}{\partial \theta_i} &= 2 \left(\frac{1}{k} \sum_i \vec{\omega_i} \right)^T \frac{\partial \left(\frac{1}{k} \sum_i \vec{\omega_i} \right)}{\partial \theta_i} \\ &= 2 \left(\frac{1}{k} \sum_i \vec{\omega_i} \right)^T \frac{\partial \vec{\omega_i}}{\partial \theta_i} \frac{1}{k} \\ &= \frac{2}{k} \left(\frac{\partial \vec{\omega_i}}{\partial \theta_i} \right)^T \vec{\rho}, \end{aligned} \tag{2}$$

where $\frac{\partial \vec{\omega_i}}{\partial \theta_i}$ is the gradient of the i^{th} contact wrench with respect to the coordinate θ_i. In vector notation

$$\begin{aligned}
\frac{\partial \epsilon}{\partial \vec{\theta}} &= \frac{2}{k} \begin{bmatrix} (\frac{\partial \vec{\omega_1}}{\partial \theta_1})^T \\ (\frac{\partial \vec{\omega_2}}{\partial \theta_2})^T \\ \vdots \\ (\frac{\partial \vec{\omega_n}}{\partial \theta_n})^T \end{bmatrix} \vec{\rho} \\
&= \frac{2}{k} W^T \vec{\rho}.
\end{aligned} \tag{3}$$

Extrema in Equation 1 (configurations where $\frac{\partial \vec{\epsilon}}{\partial \theta} = 0$) are potential grasp solutions. These extrema can occur when $\vec{\rho} = 0$ and when $W^T \vec{\rho} = 0$. The first case clearly corresponds to a null space in the grip Jacobian and therefore meets our criteria for a statically stabilizable grasp. The second case can arise in a number of circumstances. Some of the equilibrium grasp configurations for which $\vec{\rho} \neq 0$ can be stabilized by contact force modulation and others by including the effects of friction. Still others in the general formulation of Equation 3 are truly local minima and must be discarded.

In the following section, we will derive a controller that does not possess local minima for two and three contacts on regular, convex polygons. This implies that all equilibrium grasp configurations for this class of objects are valid candidate grasps.

3.1 Grasp Control Basis

Both W and $\vec{\rho}$ in Equation 3 require an expression for the contact wrench as a function of contact coordinates. This function in turn, depends directly on the geometry of the object. To represent a range of object geometries, we have developed two artificial potentials from which control may be derived. Force residual control is derived from a model of the contact wrench as a function of contact coordinates on a sphere. Moment residual control is derived from a model of contact wrenches on the surface of an infinite plane. These models yield artificial potentials with unique minima representing two canonical surface geometries designed to be a *basis* for approximating a range of object geometries.

3.1.1 Residual Force Control

The residual force controller, $\mathcal{C}_f$, is derived from a model of how contact wrenches vary on a spherical geometry as in Figure 2. If θ and ϕ are the angular coordinates on the sphere, then the corresponding object frame wrench, $\vec{w}(\theta, \phi)$, can be written:

$$\begin{aligned}
w_{fx} &= -cos(\theta)cos(\phi) & \qquad w_{mx} &= 0 \\
w_{fy} &= -sin(\theta)cos(\phi) & \qquad w_{my} &= 0 \\
w_{fz} &= -sin(\phi) & \qquad w_{mz} &= 0.
\end{aligned}$$

so that;

$$(W_\theta^T)_i = \frac{\partial \vec{w}}{\partial \theta_i} = [(sin(\theta)cos(\phi))_i, -(cos(\theta)cos(\phi))_i, 0, 0, 0, 0],$$

and

$$(W_\phi^T)_i = \frac{\partial \vec{w}}{\partial \phi_i} = [(cos(\theta)sin(\phi))_i, (sin(\theta)sin(\phi))_i, -(cos(\phi))_i, 0, 0, 0].$$

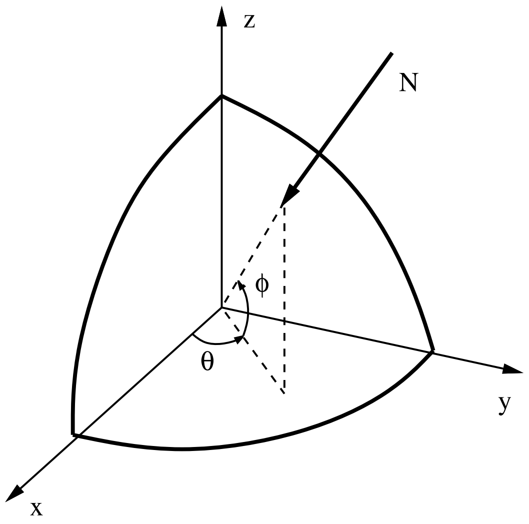

Figure 2: Local surface model for the residual force potential.

We have shown [17, 18], that controllers of the form defined by Equation 3 using these geometric constructs have a unique global minimum. Therefore, gradient descent on the residual force potential yields a unique grasp configuration.

3.1.2 Residual Moment Control

Figure 3 illustrates the geometry from which the residual moment potential is derived. The residual moment controller $\mathcal{C}_m$ minimizes the moment residual by controlling the position of the contact (r_θ, r_ϕ) on a locally planar surface defined by parameters (r_n, θ_n, ϕ_n).

Contact forces are constant everywhere on the plane and moments, $\vec{m} = \vec{r} \times \vec{f}$, vary linearly with surface coordinate, passing through zero at $(r_\theta = 0, r_\phi = 0)$. The resulting wrench model is:

$$\begin{array}{rclcrcl}
w_{fx} & = & -cos(\theta_n)cos(\phi_n) & \quad & w_{mx} & = & -r_\theta sin(\phi_n)cos(\theta_n) + r_\phi sin(\theta_n) \\
w_{fy} & = & -sin(\theta_n)cos(\phi_n) & \quad & w_{my} & = & -r_\theta sin(\phi_n)sin(\theta_n) - r_\phi cos(\theta_n) \\
w_{fz} & = & -sin(\phi_n) & \quad & w_{mz} & = & r_\theta cos(\phi_n).
\end{array}$$

This model yields correct instantaneous wrenches (and therefore wrench residuals) for all objects provided that (r_n, θ_n, ϕ_n) are known or are measurable. The moment residual controller assumes that these parameters are constant in the neighborhood of contact i, so that

$$(W_{r\theta}^T)_i = \frac{\partial \vec{w}}{\partial r_{\theta i}} = [0, 0, 0, -(cos(\theta_n)sin(\phi_n))_i, -(sin(\theta_n)sin(\phi_n))_i, (cos(\phi_n))_i].$$

and

$$(W_{r\phi}^T)_i = \frac{\partial \vec{w}}{\partial r_{\phi i}} = [0, 0, 0, (sin(\theta_n))_i, -(cos(\theta_n))_i, 0].$$

Controllers of the form of Equation 3 based on this geometry respond exclusively to moment residuals. We have shown [17, 18] that the moment residual, ϵ_m, potential function contains a single, global minimum on the infinite plane.

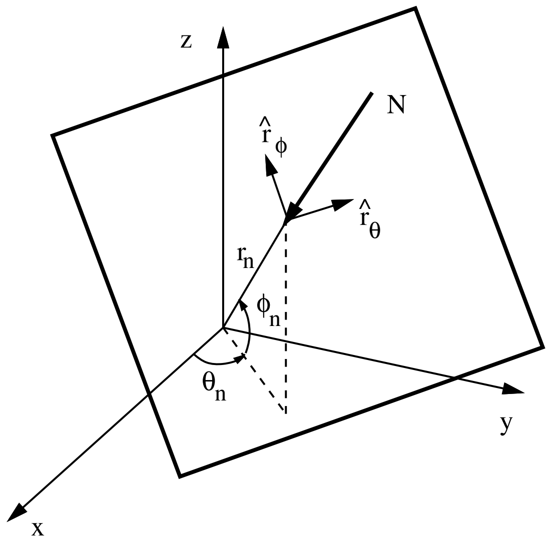

Figure 3: Local surface model for the residual moment potential.

Figure 4 shows the squared force and moment residuals for a square shape and 2 contacts. Those plots are obtained by fixing the black contact at $\theta_0 = -\pi/6$, and moving the other contact over the range $0 \leq \theta_1 < 2\pi$. Figure 4(b) identifies four minima (exactly one per face) for this object in the moment residual and Figure 4(c) illustrates the single minimum in the force residual.

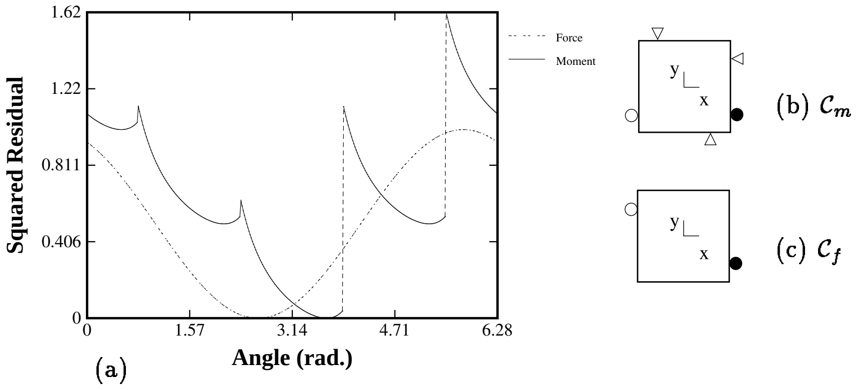

Figure 4: (a) The force and moment residuals for the planar square shape. (b) Attractors in the moment residual (one per face). (c) Unique attractor in the force residual.

Figure 4 suggests that the globally optimal configuration may be reached by first minimizing the force residual (i.e. performing gradient descent on the residual force potential), and then minimizing the moment residual. For the square shape, at least, this strategy will produce the globally optimal solution. In the next section, we will show that this is true generally for regular, convex polygons. In subsequent sections, we will show how this result can be extended to address general object geometries.

3.2 Control Composition

Given the instantaneous force residual, ϵ_f, the moment residual, ϵ_m, and a small positive force residual threshold, τ, we propose a simple composition of $\mathcal{C}_f$ and $\mathcal{C}_m$:

$$\begin{array}{rcl} \mathcal{C}^* & : & if\ (\epsilon_f > \tau)\ \ \mathcal{C}_f \\ & & else\ \mathcal{C}_m. \end{array} \tag{4}$$

This policy is implemented as a decision boundary $\epsilon_f = \tau$ on the control error plane (ϵ_f, ϵ_m). By construction, $\mathcal{C}_f$ yields a unique $\epsilon_f = 0$ grasp configuration in the plane for $k = 2$ and 3 consisting of evenly spaced contacts separated by $2\pi/k$ radians. Then, according to $\mathcal{C}^*$, $\mathcal{C}_m$ modifies this configuration to minimize ϵ_m.

To prove correctness, (a) we note that $\mathcal{C}_f$ solutions are the closest approximation to a zero force residual on regular n-gons, (b) we identify the range of $\mathcal{C}_f$ solutions possible without changing edges, and (c) we determine whether the unique $\mathcal{C}_m$ solution for these edges occurs within that range. If such a $\mathcal{C}_m$ solution is found, then it is the global minimum in the squared wrench residual since it minimizes both force and moment residuals on the n-gon.

Consider the $\phi = 0$ section of a regular polyhedra. The $\mathcal{C}_m$ controller (Equation 3) in the r_θ coordinate is written:

$$\frac{\partial \epsilon}{\partial \vec{r_\theta}} = -\frac{2}{k} W_{r_\theta}^T \vec{\rho}$$

where:

$$\begin{array}{rcl} (W_{r_\theta}^T)_i & = & [0,0,0,0,0,1] \\ \vec{\rho} & = & \sum_{i=0}^{k-1} [-cos(\theta_n), -sin(\theta_n), 0, 0, 0, r_\theta]_i \end{array}$$

Under these conditions:

$$\begin{bmatrix} \frac{\partial \epsilon}{\partial r_{\theta 0}} \\ \frac{\partial \epsilon}{\partial r_{\theta 1}} \\ \vdots \\ \frac{\partial \epsilon}{\partial r_{\theta (k-1)}} \end{bmatrix} = \frac{2}{k} \begin{bmatrix} \sum_{i=0}^{k-1} r_{\theta i} \\ \sum_{i=0}^{k-1} r_{\theta i} \\ \vdots \\ \sum_{i=0}^{k-1} r_{\theta i} \end{bmatrix} \tag{5}$$

The gradient at each contact is identical so that configuration changes produced by $\mathcal{C}_m$ move all contacts in the same direction. We have shown [17] that quadratic forms of $\mathcal{C}_f$ and $\mathcal{C}_m$ can be defined so that actions generated by $\mathcal{C}_m$ preserve $\mathcal{C}_f$ equilibria ($\epsilon_f = 0$) precisely. This is to say that $\mathcal{C}_m$ operates strictly within the null space of $\mathcal{C}_f$. This property guarantees that limit cycles cannot exist and therefore, that no spurious minima can be introduced.

Theorem 3.1 (Correctness) *For 2 and 3 contacts on regular, convex polygons, $\mathcal{C}^*$ yields the globally minimum wrench residual.*

Figure 5 illustrates a generic polygon and defines several useful geometric properties. For convenience, the edges of the polygon are numbered from 0 to $n-1$ and we assume that contact 0 is positioned on edge 0. If we further assume that contact 0 is positioned at $\theta_0 = 0$, then the coordinate of the i^{th} contact in the $\mathcal{C}_f$

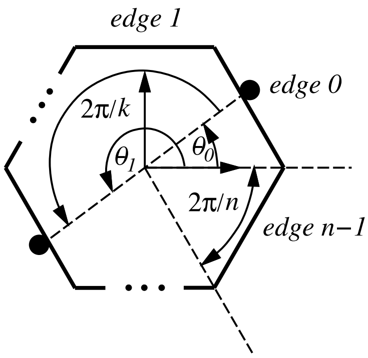

Figure 5: 2 contacts ($k = 2$) on an n-sided regular polygon.

configuration is written:

$$\theta_i = i * \frac{2\pi}{k} \qquad 0 \le i \le k-1, \quad for\ k = 2, 3.$$

When k contacts are placed on the perimeter of the regular, n-sided polygon with $\theta_0 = 0$, the remaining $k-1$ contacts occur at discrete, $2\pi/nk$ intervals on their respective edges. Using these conventions, we can establish the conditions necessary for equilibrium in $\mathcal{C}_m$. By Equation 5

$$\sum_{i=0}^{k-1} r_{\theta i} = 0 \tag{6}$$

identifies minima in ϵ_m. Two possible conditions arise.

<u>n **is an integer multiple of** k</u> In this case, all the contacts fall on vertices and the $\mathcal{C}_f$ grasp configuration may be rotated through the entire angle subtended by an edge, $2\pi/n$, without any of the contacts leaving an edge. In this circumstance,

$$\sum_{i=0}^{k-1} r_{\theta i} = \sum_{i=0}^{k-1} tan(-\frac{\pi}{n} + \psi) \Rightarrow tan(-\frac{\pi}{n} + \psi) = 0$$

where ψ is the angle through which the $\mathcal{C}_f$ configuration is moved by the $\mathcal{C}_m$ controller. It is clear that $\psi = \frac{\pi}{n}$ is a solution and that it remains within the range specified.

<u>n **is not an integer multiple of** k</u> In this case, k contacts are distributed uniformly from $[-\frac{\pi}{n}, +\frac{\pi}{n} - \frac{2\pi}{kn}]$ at $2\pi/kn$ intervals on their respective edges. In this circumstance,

$$\sum_{i=0}^{k-1} r_{\theta i} = \sum_{i=0}^{k-1} tan(-\frac{\pi}{n} + \frac{2\pi i}{kn} + \psi) = 0$$

The *tangent* function is unique and odd over this domain so that this condition is equivalent to requiring that the sum of the relative contact angles is zero:

$$\begin{aligned} 0 &= \sum_{i=0}^{k-1}(-\frac{\pi}{n} + \frac{2\pi i}{kn} + \psi) \\ &= k(-\frac{\pi}{n} + \psi) + \frac{2\pi}{kn}(\frac{k(k-1)}{2}) \\ \psi &= \frac{\pi}{kn}. \end{aligned}$$

Again, this solution is within the specified range. As in the previous case, this ϵ_m minimum is exactly midway through the range permitted. □

4 Contact Friction

The $\mathcal{C}^*$ controller optimizes the configuration of frictionless point contacts, but there is not yet any assurance that these configurations are stable in general — the analysis must consider contact friction. In this section, equilibrium grasp configurations (and their precursor states) are labeled with the minimum coefficient of friction *necessary* to produce a stable grasp.

$\mathcal{C}^*$ grasp configurations are optimal for regular, convex polygons and are statically stabilizable for appropriate contact forces and friction. The minimum required coefficient of friction, μ_0, depends on the contact configuration. The pair (ϵ_f, ϵ_m) define the current *state* of the grasp. As the $\mathcal{C}^*$ controller modifies the current contact configuration, a succession of states $\{(\epsilon_f^0, \epsilon_m^0), (\epsilon_f^1, \epsilon_m^1), \ldots, (\epsilon_f^t, \epsilon_m^t)\}$ are constructed until convergence. Upon convergence of $\mathcal{C}^*$, the minimum friction coefficient μ_0 required for the static equilibrium position is evaluated, and used to label the equilibrium state and all of its precursor states, according to equation

$$\mu^{k+1}(\epsilon_f, \epsilon_m) = \max(\mu_0, \mu^k(\epsilon_f, \epsilon_m)),$$

where k denotes the last grasping trial. The *preimage* of $\mathcal{C}^*$ is therefore a worst-case prediction for the minimum required friction coefficient after $\mathcal{C}^*$ convergence, for every accessible state (ϵ_f, ϵ_m). The construction of the preimage for the $\mathcal{C}^*$ controller is done incrementally over a number of grasping trials. In each trial, k contacts are randomly placed on the object surface from which the $\mathcal{C}^*$ controller minimizes force and moment residuals.

4.1 Minimum Required Friction Coefficient: μ_0

The minimum coefficient of friction required, μ_0, is determined by performing a binary search in the interval $[0, 1]$. Friction coefficients in this range are used to specify constraints in a mathematical programming problem that determines whether an appropriate contact force distribution exists. The search is conducted by the following algorithm:

***Compute*-μ_0** (μ_{min}, μ_{max})
    if $(\mu_{max} - \mu_{min} < \delta)$
        return (μ_{max});
    $\mu = 0.5(\mu_{max} + \mu_{min})$;
    if (***Equilibrium-Possible*** $(\mu, \vec{\Theta})$)
        return ***Compute*-μ_0** (μ_{min}, μ);
    else
        return ***Compute*-μ_0** (μ, μ_{max}).

where δ specifies the desired precision of μ_0, and $\vec{\Theta}$ is the vector of contact coordinates and normals. More efficient algorithms for identifying μ_0 are available [19]; the approach reported here was chosen for its simplicity.

The function ***Equilibrium-Possible*** $(\mu, \vec{\Theta})$ returns `TRUE` if a contact force solution exists given μ and the contact configuration. The problem is expressed as a mathematical programming problem [20, 21] subject to constraints for each contact:

1. $|\vec{f_n}| \geq +1$ — normal forces are compressive with magnitude greater than or equal to 1,
2. $|\vec{f_t}| \leq \mu|\vec{f_n}|$ — the net contact force must remain within the friction cone, and
3. $\sum \vec{f} = \sum \vec{r} \times \vec{f} = \vec{0}$.

The objective function is superfluous in this context since we are only concerned with whether the system of constraints yields a non-empty solution space. The binary search discovers the minimum coefficient of friction for which this is true.

4.2 Labeling Attractors in $\mathcal{C}^*$

Figure 6 illustrates the preimage maps for 2 and 3 contact grasps on four regular polygons. The error

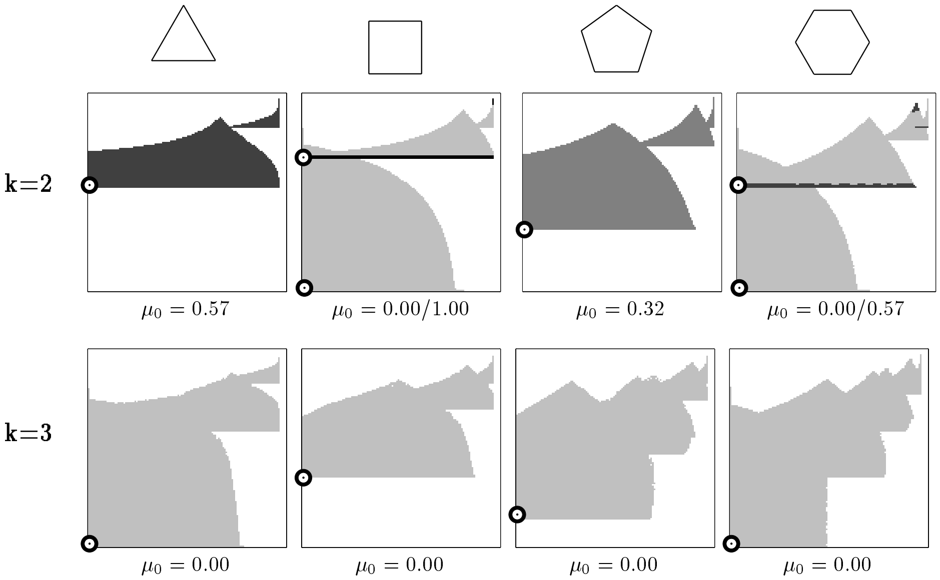

Figure 6: Labeling attractors for robust control and resource allocation.

plane is represented by a 128×128 grid. Vertical (ϵ_m) and horizontal axes (ϵ_f) are on a logarithmic scale, $log(max(\epsilon, 0.01)/0.01)$. The value for μ_0 at each cell is proportional to the grey level and is also recorded numerically under each plot; white cells are inaccessible for the given object.

4.3 Compensation and Grasp Control

Diagrams like those in Figure 6 encode the force domain signature for objects from the perspective of the $\mathcal{C}_f$ and $\mathcal{C}_m$ controllers. However, in practice, the set of attractors includes grasp configurations that are not globally optimal. One such attractor is illustrated in Figure 6 in the preimage of the square for $k = 2$, and another is evident in the preimage of the hexagon for $k = 2$. This kind of local minimum is generated by selecting a $\tau > 0$ threshold in $\mathcal{C}^*$ (Equation 4). Unfortunately, the interval between $\epsilon_f = 0$ and $\epsilon_f = \tau$ can contain a local minima. The preimage of this attractor is a set of symmetric contact configurations that lead to contacts on opposing vertices. In this configuration, $\epsilon_f < \tau$ and $\epsilon_m = 0$.

To address this case, the preimage is consulted to determine whether the "worst-case" μ_0 expected for $\mathcal{C}^*$ exceeds the contact friction specified for the task, μ_{task}. A simple but effective policy for compensation involves superimposing a small, random control action onto the $\mathcal{C}^*$ controller whenever the μ_0 label for the current grasp state exceeds the contact friction specifications for the task. When the state of the system enters the preimage of a suitable attractor ($\mu_{task} < \mu_0(\epsilon_f, \epsilon_m)$), the random control action is deactivated and $\mathcal{C}^*$ achieves this equilibrium grasp. This procedure is represented schematically in Figure 7.

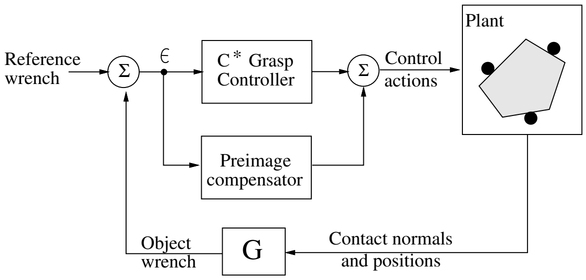

Figure 7: Compensating $\mathcal{C}^*$ using the preimage.

If we assume that during a training phase, the compensator acquires preimages for several distinguishable object geometries, then it is possible for this information to be used to guide grasp formation even when the object's identity is unknown. A composite preimage is defined:

$$\mu_0^*(\epsilon_f, \epsilon_m) = \max(\mu_0^{obj}(\epsilon_f, \epsilon_m))$$

where $obj \in \{obj_1, obj_2, \ldots, obj_n\}$, that predicts the worst-case coefficient of friction required over all candidate objects. Examples of composite preimages are presented in the left column of Figure 8. The compensator based on this composite preimage introduces randomness into the $\mathcal{C}^*$ controller whenever any of the candidate objects could lead from the current state to an inappropriate grasp configuration.

Figure 8 illustrates a typical control sequence when the task specifies a coefficient of friction of 0.1 and compensation is derived from the composite preimage. During grasp formation, (ϵ_f, ϵ_m) observations are sometimes inaccessible in some of the candidate object interpretations. At $t = 4$ and $t = 183$ in Figure 8, the observed residual, (ϵ_f, ϵ_m), is inaccessible in the $k = 2$ preimage for the objects indicated. These objects are eliminated from the set of candidate objects, changing the composite preimage and the compensation policy as well. Also at $t = 183$, after the composite preimage is updated, there are no remaining candidates for which $\mu_0 \leq 0.1$ (the $k = 2$ preimage for the triangle is labeled $\mu_0 = 0.57$). Grasp configurations for which no $\mathcal{C}^*$ attractor is expected to satisfy contact friction specifications over the set of candidate plants causes resources (additional contacts) to be introduced. Consequently, a third contact is allocated and the controller converges to a suitable grasp configuration.

5 Non-$\mathcal{C}^*$ Objects

The performance of the compensated $\mathcal{C}^*$ controller was further assessed on the set of objects depicted on Figure 9. The set of objects includes irregular polygons, piecewise smooth and concave objects in addition to regular polygons.

Figure 10 illustrates a typical grasp on a trapezoid for which $\mu_{task} = 0.1$. The left column depicts the composite preimage for the objects in the right column, given the current number of contacts. The initial grasp configuration has two contacts ($\theta = (0, \pi)$). At $t = 0$, the grasp controller eliminates the regular and the irregular triangle. Notice that for all other objects there are plausible grasp interpretations for the (ϵ_f, ϵ_m) state derived from the trapezoid.

At $t = 1$, the controller allocates a third contact (shown in white in Figure 10), at $\theta_2 \approx \pi$. At $t = 21$, the controller removes contact 0 at $\theta_0 \approx 0$ (marked with a circle in Figure 10), and subsequently eliminates the pentagon, hexagon, leaf, and the bulb object interpretations. The set of candidate objects now consists of the square and the trapezoid; the controller converges at $t = 87$ to a suitable grasp configuration, requiring

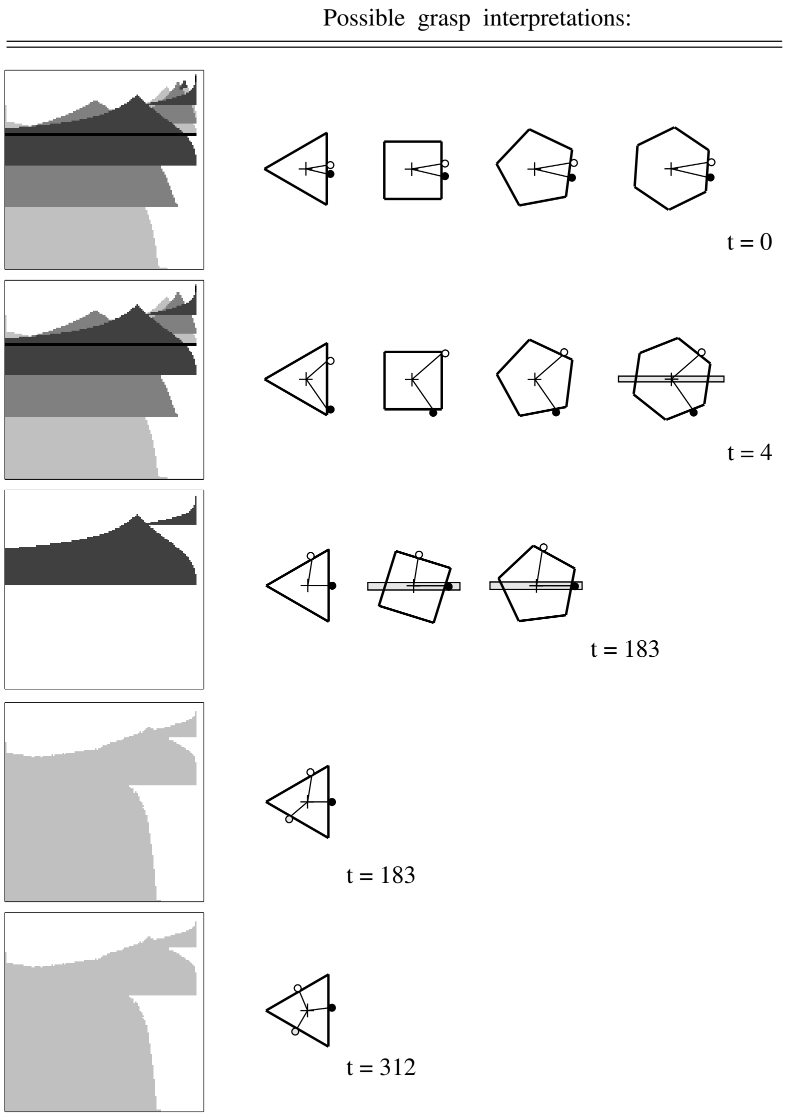

Figure 8: Adapting the policy for compensation during grasp formation.

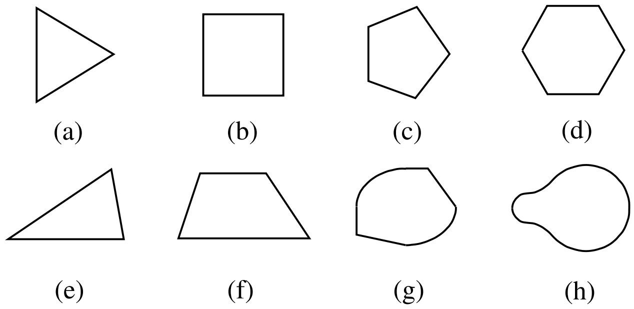

Figure 9: Set of objects used in our experiments: (a) Triangle, (b) Square, (c) Pentagon, (d) Hexagon, (e) Irregular Triangle, (f) Trapezoid, (g) Leaf, and (h) Bulb.

Table 1: System behavior with changing database size.

a friction coefficient $\mu \leq \mu_{task}$.

To investigate how the control scheme is affected by the size of the object database, we evaluated its performance over $10,000$ grasp trials. In each trial, the object to be grasped was selected from the set of 8 eight objects represented in Figure 9. Next, a database of candidate objects was chosen to include between 2 and 8 randomly selected objects. For each trial, the value of μ_{task} was set to the minimum possible value of μ_0 for the given object and the initial number of contacts (2 for these trials). For instance, the trapezoid can be grasped with a friction coefficient $\mu_0 = 0$ (contacts on top and bottom edges), or $\mu_0 = 0.44$ (contacts on left and right edges). In this case, we selected $\mu_{task} = 0.0$. This leads to the minimum number of acceptable states in the preimage (states for which the controllers are sufficient without compensation) and is consequently, a worst case performance. The compensated $\mathcal{C}^*$ controller is run until convergence, or for at most $1,000$ control cycles, when a timeout condition terminates the trial.

As shown in Table 1, the percentage of random control actions increases monotonically with the size of the database, but in an apparently sub-linear fashion. The observed increase does not affect the performance of the system, in terms of number of timeouts – in fact, the overall average for timeouts is 1.59%. There is a nearly linear increase in the number of remaining candidate objects at the end of a trial as a function of the size of the initial object database. Overall, 54% of the convergent grasps required 3 contacts, and the remaining 46% of the grasps were two-contact grasps. The system has a little bias towards producing grasps with 3 contacts.

6 Conclusion and Discussion

This paper formulates a closed-loop grasp controller in which contact feedback is used to regulate the grasp configuration. Two controllers, $\mathcal{C}_f$ and $\mathcal{C}_m$, map contact observations (positions and normals) into incremental contact displacements that minimize force and moment residuals, respectively. A composite control, $\mathcal{C}^*$, is defined as a context dependent composition of $\mathcal{C}_f$ and $\mathcal{C}_m$. We show that $\mathcal{C}^*$ is correct for 2 and 3 contacts on convex, regular polygons. The proposed approach expresses the grasp planning process in the form of multiple, asynchronous linear control processes.

The error state of the $\mathcal{C}_f$ and $\mathcal{C}_m$ controllers defines a state space representation for grasping tasks. The preimage of these controllers permits a range of possible plants (object geometries and contact resources) to be

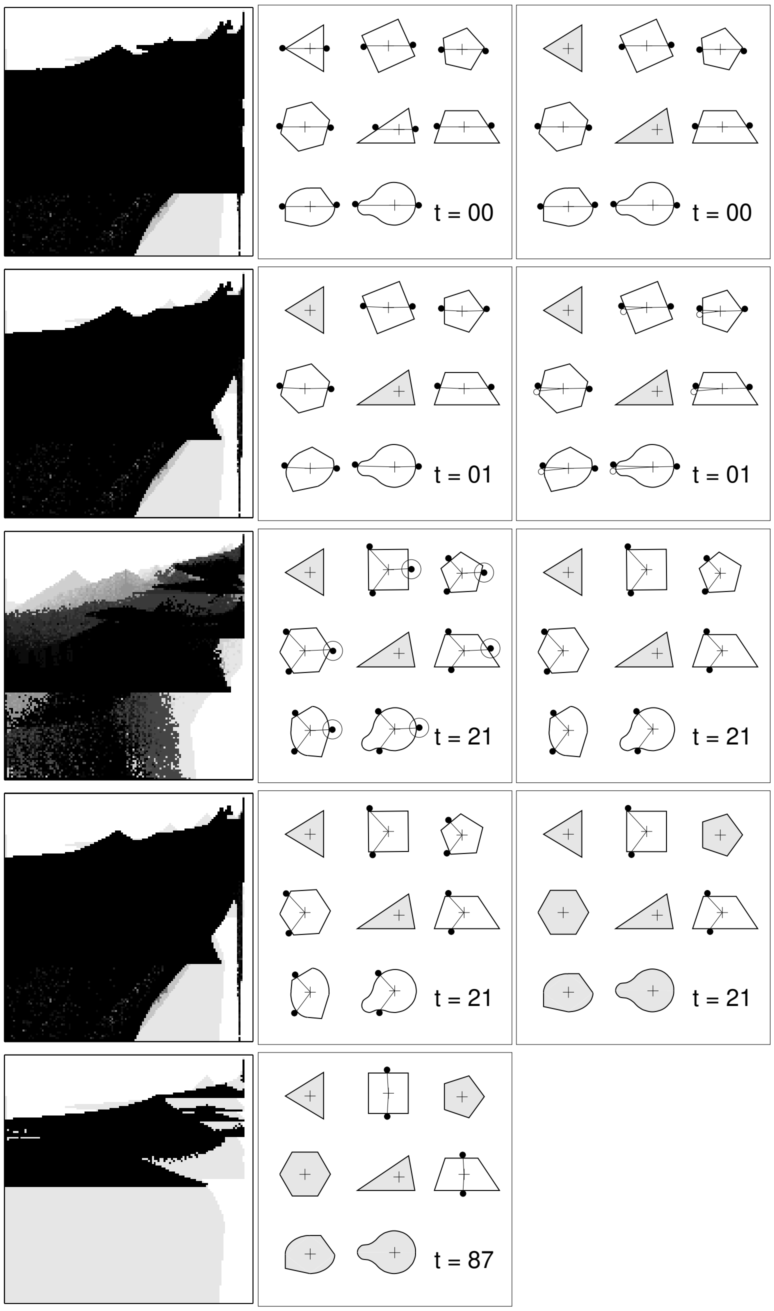

Figure 10: Grasping a trapezoid with two contacts, with $\mu_{task} = 0.1$.

distinguished and compared with respect to contact friction requirements. The $\mathcal{C}^*$ preimage is constructed over multiple exposures to a particular plant. Once built, it is the basis for a randomized compensation scheme that adapts to the stream of sensor information. We demonstrate that, properly compensated, these controllers may be applied to more general object geometries. In addition, we show how this approach supports contact resource allocation, and can be used to resolve object identity within a database of alternatives.

Enhanced Compensation Policies

The accessible states in the $\mathcal{C}^*$ preimage encode the kind of information (relative contact positions and normals) that is necessary to recognize objects on the basis of sparse, tactile data [22]. It may be possible to direct contact displacements along trajectories chosen to efficiently recognize the object. Moreover, local curvature observations can be a powerful cue for further disambiguating the object's identity. We hope to explore these issues in future extensions of this work.

The randomization method proposed executes a stochastic search, the cumulative results of which may give rise to incrementally better compensation policies. It is conceivable that better control compensation and/or recognition policies can be acquired over time by predicting the expected future reward of control actions with respect to a task specific evaluation.

It may be possible to make more effective use of the history of contact observations. For example, in Figure 10 the grasp interpretation for the square requires a significant change in the squares orientation between $t = 01$ and $t = 21$. It may be possible to eliminate grasp interpretations that do not evolve continuously over time.

3D Object Geometries, k-Contact Grasps

Both the $\mathcal{C}_f$ and $\mathcal{C}_m$ controllers are defined for 3D objects and k contacts, while the $\mathcal{C}^*$ correctness result applies only to regular, convex polygons and $k = 2$ or 3. While correctness results in 3D are much more cumbersome, these controllers preserve all the properties that such results require in 3D. In fact, we have used the full 3D $\mathcal{C}^*$ controllers in a variety of grasping and manipulation experiments in the lab.

The difficulty in extending the correctness result to $k > 3$ contacts lies in the $\mathcal{C}_f$ controller. $\mathcal{C}_f$ is designed to converge to a well defined set of contact geometries *upstream* of correct $\mathcal{C}_m$ equilibria for this class of planar object geometries. However, for $k > 3$, $\mathcal{C}_f$ does not produce a unique set of contact geometries. In practice, it may be more appropriate to activate $\mathcal{C}_m$ from contact geometries associated with kinematically well conditioned hand postures. We require that such a *preshape* controller produce a unique hand posture for a given contact geometry — formally, it must be expressed as a positive definite scalar conditioning metric. If so constructed, we may replace $\mathcal{C}_f$ with gradient descent on this scalar conditioning potential and in the preimage formulation as well. The result is an augmented notion of the plant to include the hand, the contact configuration, and the object rather than the contact and object system considered in this paper. We have constructed such a conditioning metric and will analyze this revised control basis in future work.

References

1. J. Kenneth Salisbury. *Kinematic and Force Analysis of Articulated Hands.* PhD thesis, Stanford University, Stanford, CA, May 1982.

2. B. Faverjon and J. Ponce. On computing two-finger force-closure graps of curved 2d objects. In *Proc. 1991 IEEE Int. Conf. Robotics Automat.*, volume 1, pages 424–429, Sacramento, CA, May 1991.

3. V.D. Nguyen. Constructing stable grasps. *The Int. J. Robotics Res.*, 8(1):26–37, 1989.

4. C. Ferrari and J. Canny. Planning optimal grasps. In *Proc. 1992 IEEE Int. Conf. Robotics Automat.*, volume 3, pages 2290–2295, Nice, FRANCE, May 1992.

5. Z. Li and S. Sastry. Task-oriented optimal grasping by multifingered robot hands. *IEEE Trans. Robotics Automat.*, 4(1), Feb. 1988.

6. I. Chen and J.W. Burdick. Finding antipodal point grasps on irregularly shaped objects. In *Proc. 1992 IEEE Int. Conf. Robotics Automat.*, volume 3, pages 2278–2283, Nice, FRANCE, May 1992.

7. G. Guo, W.A. Gruver, and K. Jin. Grasp planning for multifingered robot hands. In *Proc. 1992 IEEE Int. Conf. Robotics Automat.*, volume 3, pages 2284–2289, Nice, FRANCE, May 1992.

8. J.W. Jameson and L.J. Leifer. Automatic grasping: An optimization approach. *IEEE Trans. Syst., Man, Cybern.*, SMC-17(5), Sept./Oct. 1987.

9. J. Napier. The prehensile movements of the human hand. *Journal of Bone and Joint Surgery*, 38B(4), 1956.

10. M.R. Cutkosky. On grasp choice, grasp models, and the design of hands for manufacturing tasks. *IEEE Trans. Robotics Automat.*, 5(3), June 1989.

11. T. Iberall. Grasp planning for human prehension. In *Proc. IJCAI*, pages 1153–1156, 1987.

12. R. Tomovic, G. Bekey, and W. Karplus. A strategy for grasp synthesis with multifingered robot hands. In *Proc. 1987 IEEE Int. Conf. Robotics Automat.*, pages 83–89, Raleigh, NC, April 1987. IEEE.

13. N. Pollard. Synthesizing grasps from generalized prototypes. In *Proc. 1996 IEEE Int. Conf. Robotics Automat.*, volume 3, pages 2124–2130, Minneapolis, MN, April 1996. IEEE.

14. I. Kamon, T. Flash, and S. Edelman. Learning to grasp using visual information. In *Proc. 1996 IEEE Int. Conf. Robotics Automat.*, volume 3, pages 2470–2476, Minneapolis, MN, April 1996. IEEE.

15. M. Salganicoff and R.K. Bajcsy. Robotic sensorimotor learning in continuous domains. In *Proc. 1992 IEEE Int. Conf. Robotics Automat.*, volume 3, pages 2045–2050, Nice, FRANCE, May 1992.

16. H. Maekawa, K. Tanie, and K. Komoriya. Dynamic grasping force control using tactile feedback for grasp of multifingered hand. In *Proc. 1996 IEEE Int. Conf. Robotics Automat.*, volume 3, pages 2462–2469, Minneapolis, MN, April 1996. IEEE.

17. J.A. Coelho Jr. and R.A. Grupen. Control pre-imaging for multifingered grasp synthesis. In *Proc. 1994 IEEE Int. Conf. Robotics Automat.*, volume 4, pages 3117–3122, San Diego, CA, May 1994.

18. R.A. Grupen, J.A. Coelho Jr., and K.X. Souccar. On-line grasp estimator: A partioned state space approach. Technical Report COINS Technical Report 92-75, COINS Department, University of Massachusetts, Oct. 1992.

19. J.T. Schwartz and M. Sharir. Finding effective "force targets" for two-dimensional multifinger frictional grips. Technical report, Robotics and Computer Science Vision Laboratory, Courant Institute of Mathematical Science, 1986.

20. J. Kerr and B. Roth. Analysis of multifingered hands. *Journal of Robotics Research*, 4(4):3–17, Winter 1986.

21. R.A. Grupen, K. Biggers, T.C. Henderson, and S. Meek. Task defined internal grasp wrenches. Technical Report UUCS-88-001, Department of Computer Science, University of Utah, 1988.

22. W.E.L. Grimson. *Object recognition by computer : the role of geometric constraints.* The MIT Press, Cambridge, MA, 1990.